Cloning of rat amelotin and localization of the protein to the basal lamina of maturation stage ameloblasts and junctional epithelium

Pierre MOFFATT*, Charles E. SMITH*, René ST-ARNAUD†, Darrin SIMMONS‡, J. Timothy WRIGHT‡ and Antonio NANCI*[1]

*Laboratory for the Study of Calcified Tissues and Biomaterials, Faculté de Médecine Dentaire, Université de Montréal, P.O. Box 6128, Station Centre-ville, Montréal, QC, Canada H3C 3J7, †Genetics Unit, Shriners Hospital for Children, 1529 Cedar Ave., Montréal, QC, Canada H3G 1A6, and ‡Pediatric Dentistry, School of Dentistry, The University of North Carolina at Chapel Hill, Manning Dr. and Columbia St. CB#7450, Chapel Hill, NC 27599-7450, U.S.A.

Formation of tooth enamel is a very complex process in which a specific set of proteins secreted by ameloblasts play a primordial role. As part of a screening procedure to identify novel proteins secreted by EO (enamel organ) cells of rat incisors, we isolated a partial cDNA fragment (*EO-017*) that is the homologue of the recently described mouse *Amtn* (*amelotin*) gene [Iwasaki, Bajenova, Somogyi-Ganss, Miller, Nguyen, Nourkeyhani, Gao, Wendel and Ganss (2005) J. Dent. Res. **84**, 1127–1132]. Presented herein is the cloning of rat and pig full-length cDNAs with their deduced protein sequences. Detailed expression profiling by Northern-blot analysis and RT (reverse transcriptase)–PCR on rat and mouse tissues revealed highest expression in the mandible, more specifically in the maturation stage of the EO. Among all tissues tested, low expression was detected only in periodontal ligament, lung, thymus and gingiva. *In silico* analyses revealed that the *Amtn* gene is highly conserved in seven other mammals, but is absent from fish, birds and amphibians. The Amtn protein is enriched in proline, leucine, glutamine and threonine (52 % of total) and contains a perfectly conserved protein kinase CK2 phosphorylation site. Transient transfection experiments in HEK-293 cells (human embryonic kidney cells) showed that secreted Amtn is post-translationally modified possibly through O-linked oligosaccharides on threonine residues. In concordance with its predominant expression site, immunofluorescence localization within the rat and mouse mandibles revealed Amtn localized to the basal lamina of maturation stage ameloblasts of incisors and unerupted molars. Intense Amtn protein expression was also detected in the internal basal lamina of junctional epithelium in molars. The peculiar and unique cellular localization of Amtn suggests a role in cell adhesion.

Key words: ameloblast, amelotin, secretory calcium-binding phosphoprotein (SCPP), enamel organ, junctional epithelium, O-glycosylation.

INTRODUCTION

Non-collagenous matrix proteins are minor constituents in calcified tissues, yet they play very important roles in regulating both cell activity and extracellular-matrix events. In the case of enamel, the hardest calcified tissue of the body, studies aimed at elucidating the role of EMPs (enamel matrix proteins) have revealed unexpected and exciting potentials beyond structuring and organizing mineral. The EMPs comprise Amel (amelogenin), Ambn (ameloblastin) and Enam (enamelin) [1–3]. Interestingly, the genes encoding the last two are situated next to each other on the so-called SCPP (secretory calcium-binding phosphoprotein) gene cluster [4]. Among the EMPs, Amel is the most abundant secreted protein that forms supramolecular aggregates termed 'nanospheres' proposed in regulating/stabilizing apatite crystal formation [5]. The relatively low abundance Ambn and Enam are also secreted in the enamel matrix at the secretory stage, but their precise functions are currently unknown. Transgenic mice expressing mutated forms of Amel [6–8] and knockout [9] animals exhibit major enamel structural defects that seem to affect particularly the enamel rods. Loss-of-function studies have shown that Ambn and Enam are also essential for tooth formation resulting in complete absence of enamel [10,11]. Many types of amelogenesis imperfecta in humans have been attributed to mutations in those three genes [12].

Enamel formation is compartmentalized into essentially two stages, secretion and maturation. During the secretory stage, ameloblasts secrete EMPs and provide an adequate microenvironment for the formation and organization of extremely long apatite crystals. The full thickness of the enamel is laid down at this stage, but the layer is only partially mineralized. Its final characteristic hardness is subsequently achieved during the maturation stage when EMPs are lost to make space for crystal growth. Ameloblasts secrete two proteolytic enzymes, a metalloproteinase [MMP-20 (matrix metalloproteinase 20)] and a kallikrein-type serine proteinase [KLK4 (kallikrein 4)]. MMP-20 acts mainly in the short-term processing of EMPs during the secretory stage. On the other hand, KLK4 appears specifically during maturation where it is involved in the total breakdown of the remaining EMPs [3].

While matrix proteins and associated processing and degradative enzymes are clearly important to the appositional development and mineralization of enamel, there are additional and equally essential low-abundance proteins that form a thin organic layer at the interface between the apical plasma membranes of ameloblasts and the surface of maturing enamel. This layer possesses a somewhat unique developmental history, appearing in the interval of time between when ameloblasts stop appositional growth of the enamel layer (secretory stage) and initiate the series of cyclic modulations that promote its final mineralization and hardening (maturation stage). In terms of its positioning

Abbreviations used: Ambn, ameloblastin; Amel, amelogenin; Amtn, amelotin; CK2, protein kinase CK2; EMP, enamel matrix protein; Enam, enamelin; EO, enamel organ; EST, expressed sequence tag; *Gapdh*, glyceraldehyde-3-phosphate dehydrogenase gene; HA, haemagglutinin; HEK-293 cells, human embryonic kidney cells; JE, junctional epithelium; KLK4, kallikrein 4; MMP-20, matrix metalloproteinase 20; RACE, rapid amplification of cDNA ends; RT, reverse transcriptase; SCPP, secretory calcium-binding phosphoprotein.

[1] To whom correspondence should be addressed (email antonio.nanci@umontreal.ca).

and structural appearance, the layer resembles a basal lamina. Its composition, however, remains elusive, since only the presence of laminin-5 [13,14] has so far been consistently demonstrated and unlike typical basal laminae, it is rich in glycoconjugates [15,16].

Identification of all the proteins involved in the secretory and maturation stages is therefore mandatory to fully understand enamel formation. This is particularly relevant for the maturation stage where, apart from KLK4, very few genes have so far been shown to be specifically expressed [17,18]. We recently described the identification of many genes encoding soluble factors previously unsuspected to be expressed in EO (enamel organ) cells [17]. Interestingly, two of those, EO-009/APin [17,20] and EO-017 [17,21] fall within the SCPP gene cluster. While this manuscript was under preparation, Iwasaki et al. [22] reported a novel gene they called *Amtn* (*amelotin*) expressed by maturation stage ameloblasts in mouse. The EO-017 clone we had previously identified [17] is the rat homologue of this gene and will therefore be referred to herein as *Amtn*. In the present paper, we present a detailed characterization of the rat *Amtn* gene, transcripts and proteins, at the expression and immunolocalization levels.

EXPERIMENTAL

Northern-blot analysis

EOs were dissected from freeze-dried upper and lower incisors of 100 g male Wistar rats as described in [18]. Total RNA was prepared from entire EOs or from EOs that had been partitioned into secretion and maturation stages. Total RNA was extracted from all tissues using TRIzol® (Invitrogen, Mississauga, ON, Canada). The RNAs (10 or 20 μg) were electrophoresed on a Mops-buffered 1.1 % (w/v) agarose gel containing 1.2 % (v/v) formaldehyde, and transferred on to a nylon membrane (Osmonics, Westborough, MA, U.S.A.) with 20× SSC (1× SSC is 0.15 M NaCl and 0.015 M sodium citrate). After UV cross-linking, the blot was prehybridized for 2 h in Church buffer [250 mM sodium phosphate, pH 7.2, 1 mM EDTA, 1 % (w/v) BSA and 7 % (w/v) SDS] [23] at 65 °C and hybridized under the same conditions overnight with the 349 bp Amtn cDNA fragment labelled by random-priming with [α-^{32}P]dCTP (Amersham Biosciences, Baie d'Urfe, QC, Canada). The blot was washed with 0.2× SSC/0.1 % SDS at 65 °C and autoradiographed. A duplicate blot was hybridized in the same manner with a mouse Gapdh (glyceraldehyde-3-phosphate dehydrogenase) cDNA.

RT (reverse transcriptase)–PCR analyses

Total RNA extracted from various adult rat and mouse tissues was analysed with the Superscript III One-Step RT–PCR system with Platinum Taq (Invitrogen). Reactions (25 μl), typically containing 200 ng of RNA or less, were set up as per the manufacturer's recommendations. The *Amtn* gene-specific forward (5′-gcaacaaaaccgactccag-3′) and reverse (5′-ctccattctgcacatctgg-3′) primers were derived from exons 3 and 8 respectively (see Figure 3). Parallel reactions with *Gapdh*-specific primers (forward 5′-caaggtcatccatgacaac-3′ and reverse 5′-gtcattgagagcaatgcc-3′) were performed to monitor the integrity and uniformity of the RNAs. In both cases, the primers were designed from identical rat and mouse sequences. The RT–PCR conditions were as follows: 55 °C/30 min, 94 °C/2 min, followed by cycling at 94 °C/30 s, 58 °C/30 s, 68 °C/30 s and a final elongation step at 68 °C for 5 min. PCR reactions were resolved on 2 % agarose gels and stained with ethidium bromide. Anticipated amplification products for *Amtn* and *Gapdh* were of 379 and 433 bp respectively.

Cloning of rat and pig Amtn cDNAs

In order to obtain the full-length cDNA sequence for the rat Amtn, we employed a 3′-RACE (rapid amplification of cDNA ends) strategy. Briefly, the total EO RNA was first reverse transcribed with SuperscriptII (Invitrogen) and a dT_{15}-tailed oligonucleotide (5′-gagatgaattcctcgagctttttttttttttt-3′). It was then amplified by PCR with rTaq (Amersham Biosciences) and the Amtn-specific forward primer (5′-gaagtaaggtatatcatctg-3′) and the dT_{15}-tailed-specific reverse primer (5′-gagatgaattcctcgagc-3′). The porcine sequence was cloned from an EO cDNA library (a gift from J. P. Simmer, School of Dentistry, University of Michigan, Ann Arbor, MI, U.S.A.). Briefly, a primer designed to an Amtn region that is conserved between human and mouse (5′-ttctactgctttgtcttctagg-3′) was used in a PCR reaction along with an M13F vector-specific primer to amplify the 3′-end of the cDNA. The resulting amplicon sequence was used to design a second primer (5′-cctatagcaggatttagcagt-3′) that was employed to generate a 5′-RACE product. Amplification conditions were 95 °C/2 min, followed by 35 cycles of at 95 °C/30 s, 55 °C/1 min and 72 °C/3 min. The resulting products were cloned into pBluescriptKS (Stratagene, La Jolla, CA, U.S.A.) and sequenced on a CEQ2000 automated DNA sequencer (Beckman Coulter, Mississauga, ON, Canada). Sequencing results were compared with BLASTN against GenBank® non-redundant and EST (expressed sequence tag) databases. The presence of a signal peptide was verified with the SignalP V3.0 server [24].

Transient transfection in HEK-293 cells (human embryonic kidney cells) and Western-blot analysis

In order to monitor the localization of the expressed Amtn protein, the HA (haemagglutinin) epitope (ypydvpdya) was tagged at its C-terminus. Briefly, the coding portion was PCR-amplified from the rat full-length cDNA with oligos 5′-gcagaaaggtagcaaatcgaaacatg-3′ (forward) and 5′-ttacggcgcgcccttagttctatttggtgggtc-3′ (reverse). The PCR product was cloned into pCMV-Neo (Invitrogen) and linearized at the unique AscI site comprised within the reverse primer (underlined). A double-stranded linker (upper 5′-cgcgtacccatacgacgtaccagattacgctgg-3′; lower 5′-cgcgccagcgtaatctggtacgtcgtatgggta-3′) encoding the HA tag was ligated at the AscI site. The resulting plasmid was transfected into HEK-293 cells with Fugene6 (Roche, Laval, QC, Canada). Mock transfection was performed with the empty vector. The cells were washed 24 h after transfection and cultured with serum-free Dulbecco's modified Eagle's medium for another 48 h. The conditioned media and cells were then collected and processed for Western-blot analysis under denaturing and reducing conditions essentially as described in [25]. The antibody dilutions used were as follows: anti-HA (clone 12CA5; Roche) 1:1000; anti-polyHis (clone HIS-1; Sigma, St. Louis, MO, U.S.A.) 1:1000, anti-Amtn (1:1000), goat anti-rabbit and anti-mouse horseradish peroxidase conjugates (Sigma) 1:30 000. The signal was visualized by chemiluminescence with ECL® Plus reagent (Amersham Biosciences).

Antibody production

A peptide (GG^{143}QTGAKPDVQNGALPTRQ^{160}GGC) corresponding to residues 143–160 of the rat Amtn protein was synthesized. The Amtn peptide sequence was flanked by three extra glycine residues (underlined), and a C-terminal cysteine residue that served for conjugation to activated keyhole-limpet haemocyanin with maleimide. The peptide–carrier complex was mixed with complete Freund's adjuvant and injected into rabbits according to standard methods (Affinity Bioreagents, Golden, CO,

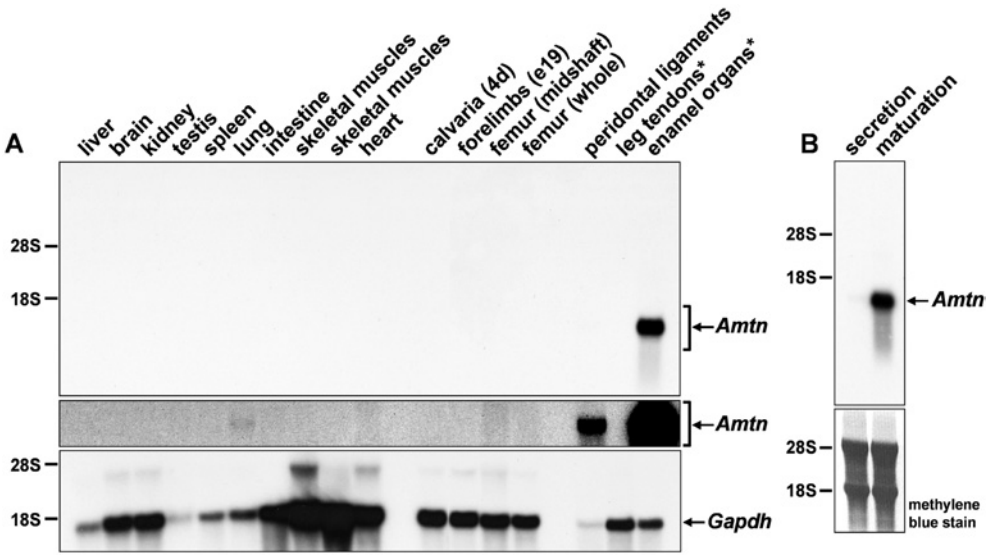

Figure 1 Northern-blot analyses of the expression of *Amtn* in rat tissues

Total RNA was extracted from tissues of adult rat unless otherwise indicated (4d: 4-days-old; e19: embryo at day 19). Either 10 μg (*) or 20 μg of RNA was separated on agarose gels and processed for hybridization. Integrity of RNA was monitored by hybridization with a *Gapdh* probe (**A**, bottom panel) or after staining the membrane with Methylene Blue (**B**, bottom panel). RNA isolated from EOs at the secretion and maturation stages of development was analysed separately (**B**). In (**A**), the middle panel is a longer exposure of the same blot shown in the top panel (bracketed area), and illustrates weaker *Amtn* expression levels present in periodontal ligament and lung. The positions of 28 S and 18 S ribosomal RNAs are indicated.

U.S.A.). The specific IgGs were purified on an epitope affinity resin generated with the same peptide as used for immunization.

Immunolocalization of Amtn in rat and mouse teeth

Male Wistar rats were anaesthetized and perfusion-fixed with paraformaldehyde–glutaraldehyde in PBS [2]. Various organs were dissected and left immersed in fixative for 24 h at 4 °C. Soft tissues were immediately processed for embedding in paraffin. Hard tissues were decalcified at 4 °C in a 4.13 % (w/v) Na_2-EDTA solution (pH 7.4) for 14 days before being processed for paraffin embedding. Thick sections (5 μm) were cut and mounted on poly+ glass slides. Sections were deparaffinized, rehydrated, and blocked in PBS containing 5 % (w/v) skimmed milk for 1 h. Sequential incubations with the Amtn antibody or a purified rabbit anti-IgG antibody followed by a secondary goat anti-rabbit Alexa Fluor® 594 antibody (Molecular Probes, Eugene, OR, U.S.A.) were performed with 1:500 dilutions in PBS at room temperature (23 °C) for 3 and 1 h respectively. After each incubation, the slides were washed three times for 10 min each with PBS-Tween [PBS containing 0.05 % (v/v) Tween 20, pH 7.4]. Nuclei were stained with 10 μg/ml Hoechst 33342 (Molecular Probes) in PBS and mounted with ProLong Gold antifade reagent (Molecular Probes). Fluorescence was examined under a Zeiss Axiophot microscope (Carl Zeiss Canada) equipped with an Olympus PD70 digital camera.

Some decalcified rat incisors were used to prepare EO caps from mid and late maturation for pre-embedding immunogold labelling with anti-Amtn as described previously [15,16]. Decalcified molars were also used to prepare gingiva exposing the JE (junctional epithelium) for labelling. Some caps were processed for observation in a JEOL 7400F field emission scanning electron microscope using backscatter imaging, while others, together with gingival samples, were processed for visualization with a JEOL 2011 transmission electron microscope. After blocking for 15 min with PBS containing 5 % milk, the samples were incubated in PBS with the anti-Amtn antibody or with a purified rabbit IgG (each at 1:750) overnight at 4 °C, washed and then incubated with Protein A–gold conjugate at room temperature for 1 h.

RESULTS

Expression profiling of *Amtn* in rat tissues and *in silico* analyses

In the course of screening a library from rat incisor EOs for cDNA fragments encoding signal peptides [17], a clone called EO-017 (Amtn) was found and is further characterized herein. Initial BLAST searches at GenBank® Nucleotide Sequence Database indicated the full-length human (NM_212557) and mouse (XM_284166) sequences had been identified, but no information was available for the rat. Also, very limited information could be inferred as to the expression site for this gene, as the total number of ESTs inventoried at UniGene was low [three for the human (Hs.453069) and seven for the mouse (Mm.79700)]. Northern blotting experiments were conducted in order to better define the rat *Amtn* gene expression pattern on a set of 17 different rat RNAs. The results obtained indicated the presence of a single transcript at roughly 1.1 kb (Figure 1A). Among the tissues tested, expression of *Amtn* was very high in EOs, low in periodontal ligaments, and virtually absent in all other tissues examined (Figure 1A, top panel). Upon longer autoradiographic exposures, however, a very faint signal was also detected in lung (Figure 1A, middle panel). The site of expression of the *Amtn* gene was further refined on RNA samples extracted from separate functional regions of the EO. The *Amtn*-specific signal was high in samples from maturation stage and barely detectable in those from secretion stage (Figure 1B).

Cloning of the full-length cDNA for rat Amtn and deduced sequences

In order to gain more information on the protein encoded by the rat *Amtn* gene, its full-length cDNA was cloned. The cloning procedure yielded three different transcripts, with the longest

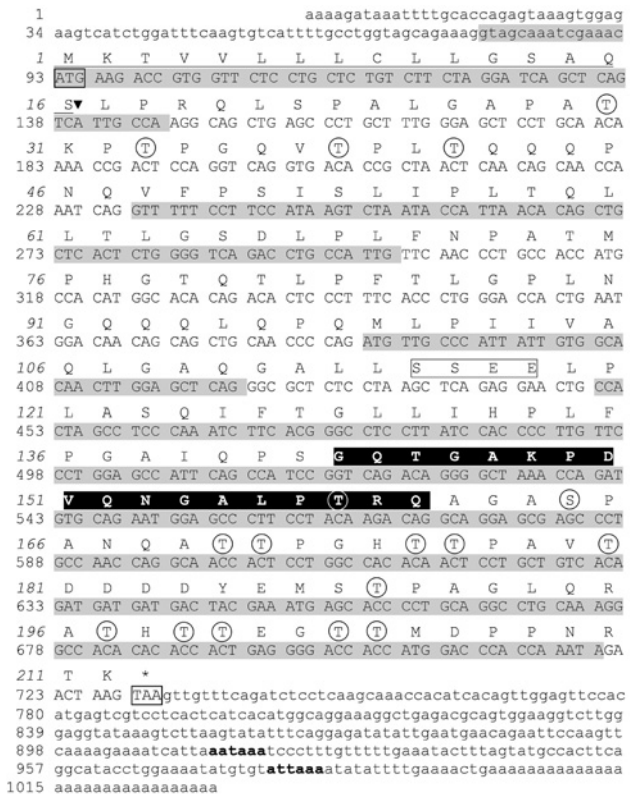

Figure 2 Full-length cDNA for rat *Amtn* and its deduced protein sequence

The normal and italicized numbers at left refer to the nucleotide and protein sequences respectively. The 5′- and 3′-untranslated regions are in lower-case, and the coding region is in upper-case. The start and stop codons are boxed and two polyadenylation signals are shown in boldface. The nucleotides corresponding to different exons are depicted by alternating white/grey shadings. The signal peptide is underlined and a downward arrowhead indicates its predicted cleavage site. A putative CK2 serine phosphorylation site (SSEE) is boxed, and the peptidic sequence used for antibody production is highlighted black. Predicted O-glycosylated serine and threonine residues are circled.

containing 1032 nt (Figure 2) (GenBank® accession number DQ198381; [17]). This cDNA most likely matches the size of the abundant transcript detected by Northern-blot analysis (Figure 2). The two others represent splice variants, as transcript 2 was missing exon 7 only, while transcript 3 lacked exons 3–7 (see Figure 3D). The longest Amtn cDNA has a single open reading frame starting at an adequate Kozak consensus ATG (nt 93) extending to a stop codon at nt 729 (Figure 2). The translated protein was composed of 212 residues, including a predicted cleavable signal peptide (Figure 2, downward arrowhead). Features of the resulting Amtn mature protein (devoid of signal peptide) include a computed pI of 5.4, the absence of cysteine residues, and the roughly equal abundance of proline, leucine, glutamine and threonine (52 % of total by weight) (Figure 2). Inspection of the polypeptide sequence for predicted post-translational modifications revealed the presence of only a consensus CK2 (protein kinase CK2) phosphorylation site (SXXE where X represents any amino acid) present at Ser^{115} (Figure 2, boxed) and several putative O-glycosylation sites (Figure 2, circled). None of the six asparagine residues were predicted to be N-glycosylated. The two other transcripts encoded shorter proteins (203 and 111 residues for transcripts 2 and 3 respectively) still containing a signal peptide (Figure 3D). Interestingly, transcript 2 lacks the CK2 phosphorylation domain encoded by exon 7.

To gain more information on the genomic organization of the rat *Amtn* gene, and to be able to derive sequences from other species, BLAST homology searches were performed through Ensembl [26]. The *Amtn* gene was found to be located on rat chromosome 14 (p21 band) (Figure 3A) in a cluster rich in genes encoding secreted proteins (Figure 3B) which are all in the same orientation, including its immediate neighbours mucin 10 (*Muc10*) (50 kb upstream) and the tooth-specific genes *Ambn* (35 kb downstream) and *Enam*. The *Amtn* gene spans approx. 12 kb and is composed of nine exons, which are all coding except exon 1 (Figure 3C). The first seven coding exons are phase 0, meaning that codons are not interrupted by exon–intron boundaries (see Figure 2). Protein sequences from seven other species were inferred from the available genome sequences (chimp, macaque, dog and opossum) or from existing EST (cow) and cDNA (human and mouse). The porcine protein was also deduced after cloning its sequence from an EO cDNA library (GenBank® accession number was unavailable at time of submission). Protein alignments indicated that Amtn is conserved in mammals, with an overall identity of 26 % and similarity of 50 % (Figure 4). The highest degree of similarity was found between the human, chimp and macaque (90 %), the bovine, pig and dog (70 %), and the rat and mouse (88 %). The overall protein features described above for the rat were also present in the other species including the conserved presence of a signal peptide (Figure 4, underlined) and of the putative CK2 phosphorylation site (Figure 4, boxed). The *Amtn* gene does not appear to be present in chickens, fish (fugu, tetraodon and zebrafish), and amphibians (salamander and xenopus).

SDS/PAGE of secreted Amtn indicate it is post-translationally modified

To assess the secretion and to determine whether the Amtn protein is post-translationally modified, it was detected by Western-blot analysis after transient transfection in HEK-293 cells. After 48 h, the C-terminally HA-tagged rat Amtn protein was chiefly detected in the conditioned media produced by transfected cells, but not in the cell extracts (Figure 5, arrow). No specific signal was detected in mock-transfected cells and corresponding conditioned media (Figure 5). The Amtn protein-specific signal was very diffuse and broad, migrating just below the 37 kDa marker. This was roughly 10–15 kDa greater than the theoretical size for the unmodified rat HA-tagged Amtn protein (21.8 kDa). In contrast, a bacterially produced recombinant His_6-tagged Amtn migrated exactly at its expected molecular mass of 21.2 kDa (Figure 5, arrowhead). An almost identical migration behaviour was observed with the untagged native rat Amtn protein (results not shown). These results confirm that the Amtn protein is post-translationally modified.

Amtn is expressed at highest levels in mandible in the rat and mouse

RT–PCR analyses performed on rat and mouse tissues confirmed and extended the Northern-blot analyses. The oligos used were designed from identical regions in exons 3 and 8 of the rat and mouse (see Figure 3D). In rat tissues, a specific Amtn product was faint but chiefly detectable in lung and periodontal ligaments, whereas it remained undetectable in tongue, thymus, spleen and pancreas (Figure 6A). Strongest signals were detected on whole mandible and maturation stage EOs (Figures 6A and 6B). Relative levels of expression in lung and periodontal ligaments were at least 20 and 200 times lower than in maturation stage EOs respectively (Figure 6A). In mouse tissues, a strong signal was detected in RNA extracted from whole mandibles, and a very faint signal at the correct size in gingiva and thymus, but not in lung (Figure 6C).

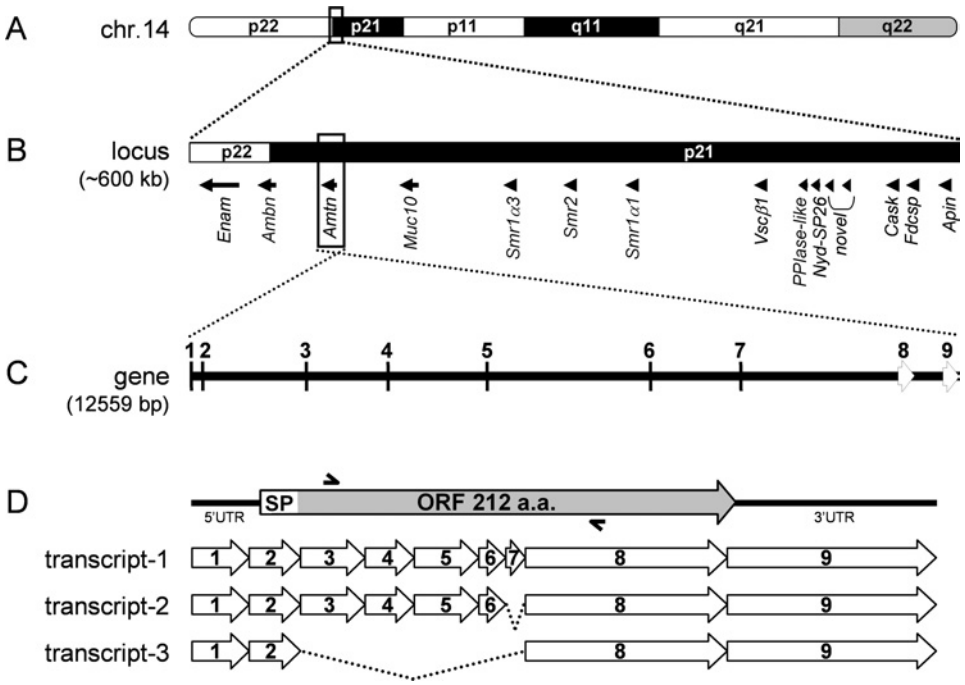

Figure 3 Schematic representation of the location and structure of the rat *Amtn* gene and its derived transcripts

The rat *Amtn* gene is located on chromosome 14 (**A**) flanked by the enamel-specific genes *Ambn* and *Enam*, and the salivary gland *mucin 10* (*Muc10*) (**B**). The 600 kb locus containing *Amtn* is rich in genes encoding secreted proteins such as the *submandibular glands androgen regulated* genes (*Smr*) and at the other extremity *casein kappa* (*Cask*), *follicular dendritic cells secreted peptide* (*Fdcsp*) and *APin* (**B**). The *Amtn* gene is composed of nine exons covering roughly 12 kb (**C**). The three different transcripts identified are depicted with the matching exons location (**D**). Semi-arrowheads above and below the longest cDNA (**D**) indicate location of the primers used for RT–PCR (Figure 5). ORF, open reading frame; SP, signal peptide. 5′UTR, 5′ untranslated region.

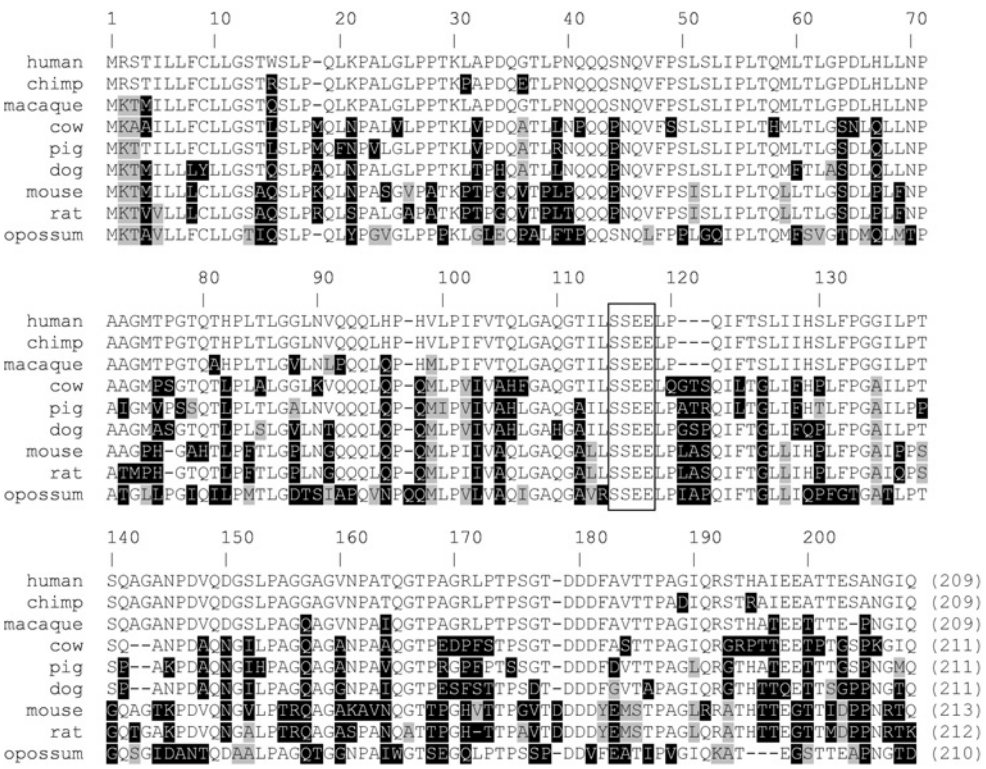

Figure 4 Alignment of the Amtn protein sequences from various mammalian species

Numbering at top refers to the human sequence, while those at the end of each sequence indicate the total number of residues in each protein. Non-identical residues are highlighted in black, and similar residues are highlighted in grey. Sequences were obtained from GenBank® entries AY358528 (human), CN440607 (cow) and AK017352 (mouse), or adapted from Ensembl transcript ENSCAFT00000004283 (dog), ENSMODT000000015781 (opossum), ENSPTRT00000030049 (chimp) and ENSMMUT00000004282 (macaque). The signal peptide (underlined) and predicted CK2 phosphorylation site (boxed) are conserved among all species.

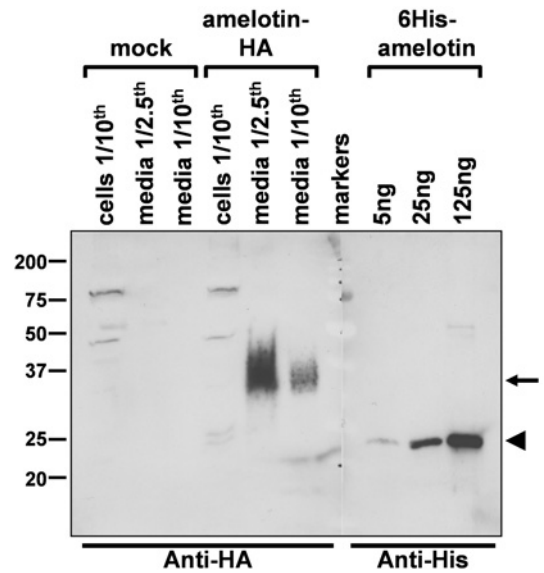

Figure 5 The rat Amtn protein is secreted into the culture media of transfected HEK-293 cells

The rat Amtn cDNA, tagged at its C-terminus with the HA epitope, was transiently transfected into HEK-293 cells. After 48 h, media and cells were collected and analysed by Western blotting with an anti-HA antibody. Proportion of samples loaded relative to total is indicated. Cells transfected with the empty vector (mock) served as control. The Amtn-specific band was detected in the conditioned media (arrow) attesting to its secretory nature. A recombinant rat His_6-tagged Amtn (6His–Amtn) was produced in and purified from bacteria by Ni-affinity chromatography. The His_6–Amtn was detected with an anti-His monoclonal antibody (arrowhead). Note the higher apparent molecular mass (35 kDa) of the mammalian Amtn protein relative to the recombinant form (22 kDa). Molecular masses (kDa) are given on the extreme left.

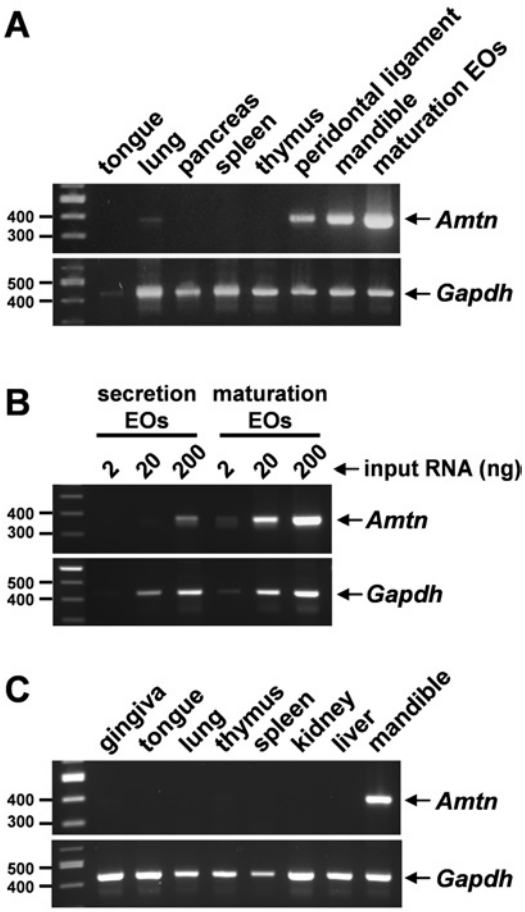

Figure 6 RT–PCR analyses of *Amtn* gene expression in rat and mouse tissues

Total RNA was extracted from adult rat (**A**, **B**) and mouse (**C**) tissues and used in one-step RT–PCR reactions. Unless otherwise specified, 200 ng of RNA was used per reaction. The PCR products were resolved on 2% agarose gels and stained with ethidium bromide. *Amtn* gene-specific primers produce a band at 379 bp. *Gapdh* primers, yielding a 433 bp product, were used in parallel reactions to assess the integrity and uniformity of the RNAs. PCR reactions were stopped after 35 cycles (**A**, **C**) and 24 cycles (**B**) for *Amtn*, and after 25 cycles for *Gapdh*. A 100 bp DNA ladder was used as markers. Molecular size (bp) is given on the extreme left.

Immunolocalization of Amtn in rat and mouse teeth

An antibody raised against an Amtn peptide (highlighted black in Figure 1) allowed us to determine the localization of the protein within the rat and mouse hemi-mandibles. Immunofluorescence images presented in Figure 7(A) illustrate localization of the Amtn protein in the rat lower incisor. Specific immunofluorescence signal only became visible starting in ameloblasts undergoing post-secretory transition (Figures 7B and 7C). In the later region, a Golgi-like labelling was transiently observed (Figures 7C and 7D), which tapered off rapidly as ameloblats progressed more into maturation (Figure 7E). At about the same time, the Amtn signal appeared as a discrete line located at the interface between the ameloblasts and the enamel layer (Figure 7D, arrowheads). The intensity of the signal at the apex of the ameloblasts increased and began to appear also on the enamel surface as it detached from the cells layer (Figure 7E). Noteworthy was the complete absence of staining over the enamel layer (Figures 7A–7E). Underlying papillary layer cells and connective tissue cells, as well as bone matrix cells (results not shown), were also unreactive (Figures 7A–7E). Serial sections incubated with a control rabbit IgG were devoid of specific signal (Figure 7I). The EO from unerupted 3rd molars still undergoing enamel development also presented a strong labelling at the apex of the ameloblasts (Figures 8A and 8B). A similar labelling pattern was observed on rat maxillary incisors (results not shown) and mouse mandibular incisors (Figures 7F–7H). Another site where an Amtn labelling was detected was on the JE of interdental papilla in rat and mouse (Figure 8). Like the signal observed in the EO, the rat and mouse JE labelling appeared as a thin line at the interface between the cells and the enamel space most probably corresponding to the internal basal lamina (Figures 8C–8G). The Amtn protein localization extended only for a short distance from the cemento-enamel junction into the JE. Again, no specific signal was detected when a rabbit IgG was used as the primary antibody (Figure 8H). Among 13 other tissues tested (liver, stomach, spleen, heart, pancreas, kidney, brain, intestine, testis, spleen, lung, salivary glands and stomach), none showed Amtn positive immunoreactivity (results not shown).

In the maturation zone of rodent incisors, there is a region where enamel is completely soluble in EDTA (see Figure 7A) thereby exposing a basal lamina that sits at the interface between ameloblasts and enamel [2,15]. Immunogold labelling confirmed that at least part of the immunofluorescence labelling for Amtn along the surface of maturation stage ameloblasts is associated with this structure (Figures 9B and 9C). Similarly, colloidal gold particles were observed over the internal basal lamina of the rat JE (Figure 10A). With both EO caps and gingival samples, labelling is restricted to the surface, since only the outer face of the basal lamina is exposed in such preparations. There were almost no gold particles associated with the basal lamina in both the EO (Figure 9D) and JE under control incubations (Figure 10B).

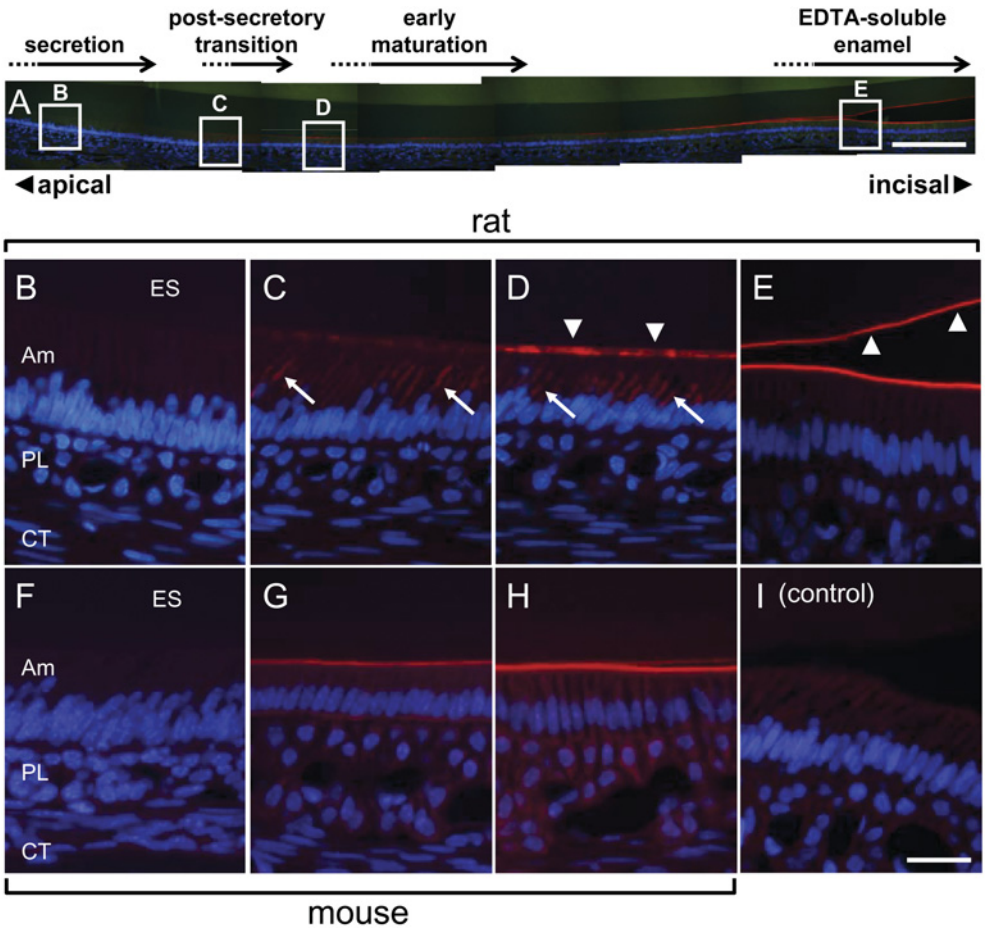

Figure 7 Immunofluorescence localization of Amtn protein in rat and mouse mandibular incisors

Composite image showing Amtn immunofluorescence localization over a 3-mm-long segment of the rat lower incisor EO (**A**). Pictures in (**B**–**D**) are magnified regions boxed in (**A**) (from left to right respectively). No specific signal is visible in secretory stage ameloblasts in rat (**B**) and mouse (**F**). Golgi-like staining is apparent in post-secretory transition (**C**, arrows), and early maturation stage ameloblasts (**D**, arrows). Prominent labelling is observed at the basal lamina-like structure along the interface between the maturation stage ameloblasts and the developing enamel (**D**, **E**, arrowheads). The enamel surface is immunoreactive where the cell layer splits away from the enamel surface as a result of sectioning (**E**). The mouse lower incisor (**F**–**H**) shows a similar pattern of Amtn labelling, being detectable at basal lamina-like surface only in the post-secretory (**G**) to maturation regions (**H**). Control incubations performed with a purified anti-rabbit-IgG on a serial section like that shown in (**E**) remained unlabelled (**I**). Scale bars, 200 μm (**A**) and 25 μm (**I**). Sections were counterstained with Hoechst (blue). Green coloration is tissue autofluorescence. ES, enamel space; Am, ameloblasts; PL, papillary layer; CT, connective tissues.

DISCUSSION

In a previous study, we applied a signal-trap strategy to identify membrane-associated proteins and proteins secreted by rat EO cells, and found some novel genes and many unanticipated known genes [17]. Here, we further characterized one of the clones that was identified (EO-017), and which corresponds to the rat homologue of the recently described mouse *Amtn* gene [22]. Northern-blot analyses revealed that the rat *Amtn* gene is highly expressed in maturation stage EOs and immunolabelling confirmed its synthesis by ameloblasts. This finding is consistent with the *in situ* hybridization results of Iwasaki et al. [22] showing expression of *Amtn* by maturation stage ameloblasts in mouse incisors and molars. We further demonstrate that *Amtn* expression is not restricted to the tooth but is also expressed, albeit at low levels, in other tissues such as periodontal ligament, lung, gingiva and thymus. This broader distribution is in concordance with the tissue origin of Amtn ESTs previously listed for mouse (Mm.79700). Two of these ESTs were identified from thymus and three from head and/or maxilla and mandible. Limited expression data for human (Hs.453069, three ESTs total) suggest that *Amtn* could also be expressed at other sites like brain and optic nerve. The maturation stage-specific expression pattern of *Amtn*, however, is quite distinct from that of *Ambn* and *Amel*, which are mainly expressed by secretory stage ameloblasts [3].

The rat chromosomal locus for *Amtn* is rich in tooth- and bone-specific genes, which have been the subject of much attention [4,19,21,27,28]. The genes present on this cluster encode the so-called SCPP [4], of which *Amtn* has recently been classified a member [21]. The chromosomal location of the *Amtn* gene upstream of *Ambn* in all species identified to date, as well as the highly similar gene organization, indicates that they are homologues. Further, the protein sequence alignments derived from nine different mammal species, including pig Amtn, display an overall high homology. The fact that Amtn seems to be absent in birds, fish and amphibians suggests that it might have evolved from an ancestral gene to serve a more specialized role in teeth of mammals. All protein sequences contain a *bona fide* signal peptide with a cleavage site after Ser^{16} that has been experimentally verified by microsequencing of the human Amtn protein expressed in mammalian cells [29]. Predictive tools [30,31] reveal only the usual low-expectation-value post-translational modifications such

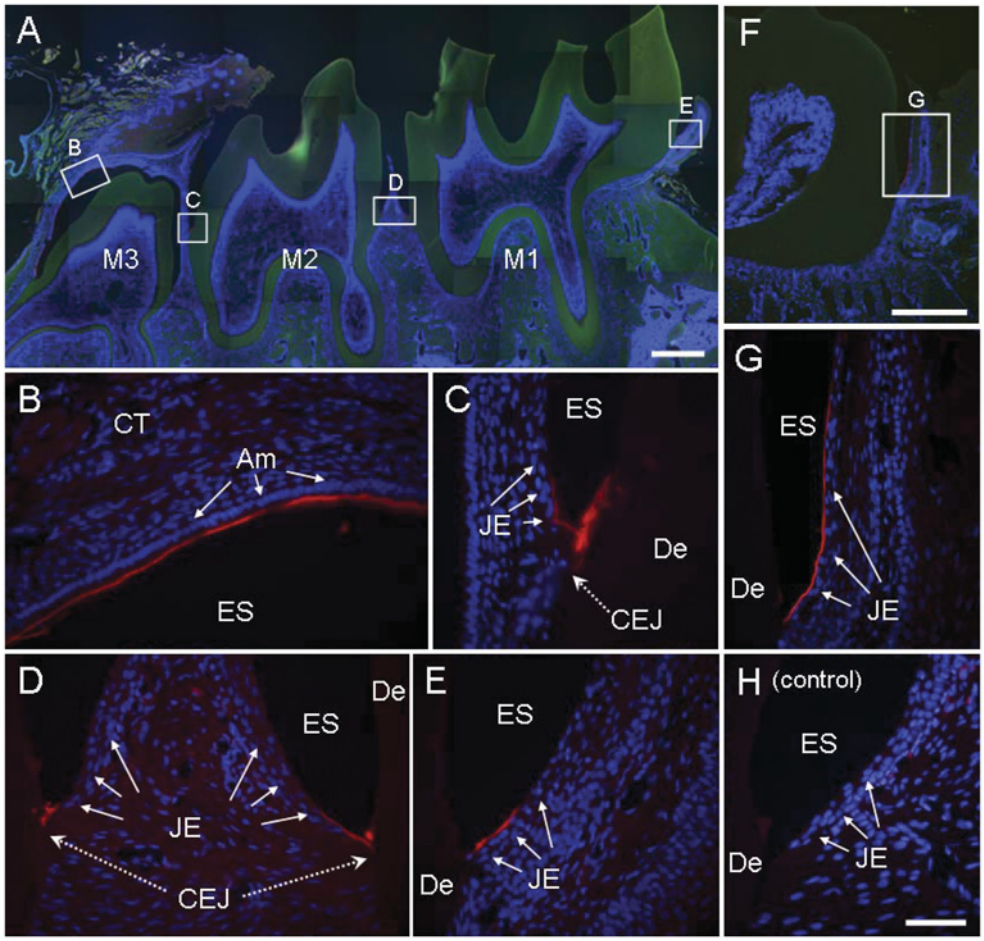

Figure 8 Immunofluorescence localization of Amtn on rat and mouse mandibular molars

Composite image showing Amtn immunofluorescence in rat (**A**) and mouse (**F**) molars. Boxes in (**A**) and (**F**) represent areas enlarged in (**B**–**E**) and (**G**) respectively. Amtn labelling is present at the basal lamina-like surface of the rat unerupted molar (**B**). Detection of Amtn at the internal basal lamina of JE in first and second molars in rat (**C**–**E**) and mouse (**G**). Control incubation performed with a purified anti-rabbit-IgG on a serial section as that shown in (**E**) remained unlabelled (**H**). Scale bars, 500 μm (**A**), 250 μm (**F**) and 25 μm (**H**). Sections were counterstained with Hoechst (blue). Green coloration is tissue autofluorescence. ES, enamel space; Am, ameloblasts; De, dentin; CEJ, cemento-enamel junction.

as serine/threonine phosphorylation and O-glycosylation, but no obvious motifs or domains known to be present in other proteins, suggesting that Amtn is unique and not part of a family.

A consistent finding of the present study was the dramatic shift in migration of Amtn secreted by HEK-293 cells relative to its unmodified recombinant counterpart. Considering the increase in mass detected by SDS/PAGE (10–15 kDa), and also its broad migration pattern, it can be estimated that Amtn could bear up to ten O-linked sugar moieties. This would be consistent with the presence of several threonine residues mainly clustered in the C-terminal half of the protein that are in a favourable sequence context for O-glycosylation [32,33]. Because most of these residues are conserved among mammals, they represent strong candidate sites for modification. In addition, the apparent shift in the molecular mass of Amtn is unlikely to be due to aberrant migration behaviour inherent to the primary sequence, as the unmodified bacterial recombinant form matches that of its deduced theoretical size. These results contrast with those of Iwasaki et al. [22], who have shown that overexpression in C2C12 cells of the $3 \times$ FLAG epitope-tagged Amtn produced a 28 kDa protein that was indistinguishable between media and cell extract. They concluded from this result that Amtn undergoes no significant post-translational modifications. A possible explanation for this discrepancy is the different cell lines used. As there are very few, if any, relevant *in vitro* cell models that fully mimic ameloblast physiology, detection and analysis of Amtn extracted directly from teeth should resolve this issue.

The putative phosphorylation of Amtn at the conserved CK2 site (SSEE), present in every species analysed so far, might have a functional implication. This is particularly interesting in view of the two splice variants that we have shown, and which would encode truncated proteins lacking the CK2 domain. It is tempting to speculate that this would extrapolate into fundamental differences in the function of the various isoforms of Amtn, as is the case for some heavily phosphorylated molecules (osteopontin, dentin matrix protein-1 and phosphophoryn) involved in biomineralization of tooth and bone [34–36]. The contribution of phosphorylation to the migration behaviour of mammalian Amtn on SDS/PAGE, however, would be minimal, as it adds only 80 Da per phosphate moiety. Supportive evidence for this was obtained from transient expression experiment in HEK-293 cells where the protein produced by transcript-2 was similar to that of the full-length transcript, irrespective of the presence of the HA epitope (results not shown).

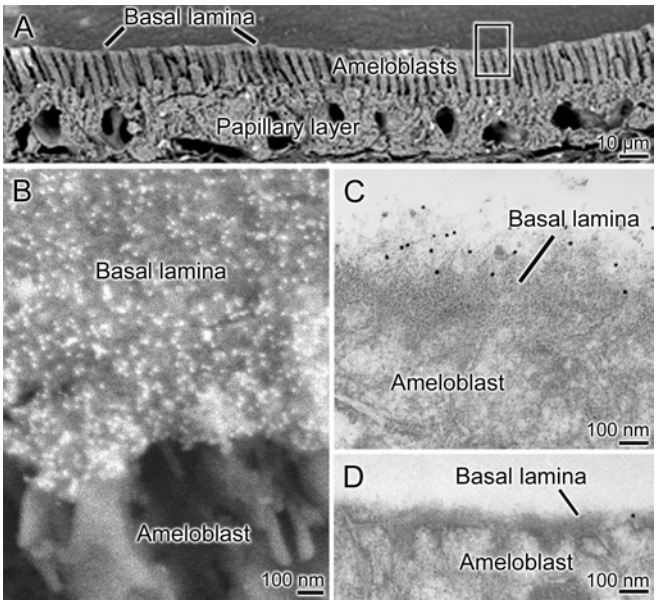

Figure 9 High-resolution immunolocalization of Amtn to the basal lamina of rat maturation stage ameloblasts

Low-magnification, scanning electron micrograph of an EO cap showing the ameloblast layer and a surface view of the overlying basal lamina (**A**). Backscattered electron imaging of the immunogold labelling for Amtn in a region similar to the boxed area in (**A**) is shown in (**B**). The pattern of distribution of gold particles, which appear as white particles with this type of imaging, indicates that Amtn is distributed throughout the basal lamina (**B**). Transmission electron micrographs of EO caps labelled for Amtn (**C**) and incubated under control conditions (**D**). The basal lamina appears as an electron-dense layer at the ameloblast apex decorated at its surface with gold particles, which appear black in transmission microscopy. The control shows virtually no gold particles.

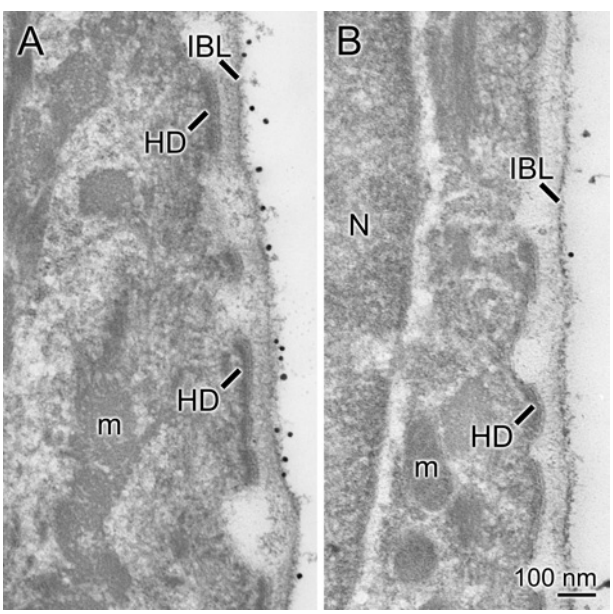

Figure 10 Immunogold localization of Amtn to the internal basal lamina (IBL) of the rat JE

Transmission electron micrographs showing the presence of Amtn over the inner basal lamina (IBL) (**A**) and the almost complete absence of gold particles under control conditions (**B**). HD, hemidesmosome; m, mitochondria, N, nucleus.

Immunohistochemical localizations of Amtn in tissue sections with a peptide-specific antibody revealed an interesting and unique localization pattern in two distinct yet developmentally related cell types in both rat and mouse. First, and most dramatic, it was found in maturation stage ameloblasts, as was anticipated from the expression data published by Iwasaki et al. [22]. Detection begins in post-secretory transition and, in incisors, extends to the gingival margin. The secreted protein accumulates at the interface between the apical extremity of ameloblasts and the enamel surface throughout maturation. The apical labelling persisted throughout maturation, but Golgi labelling, however, was only clearly discernable during early maturation. This suggests that the protein may be quite stable once secreted, and/or its message is translated at very low levels later in maturation. Amtn is clearly not an EMP, since it is not immunodetected to any significant level in the enamel layer.

Concentration of ameloblast-specific proteins at their apical surface during the maturation stage has so far not been reported. The interface between maturation stage ameloblasts and the enamel is characterized by the presence of a basal lamina-like structure. Except for an abundance of specific sugars not typically seen in basement membranes and laminin-5, this structure remains poorly defined at the molecular level [16,37]. Immunostaining for Amtn was conspicuously localized to the basal lamina, thereby establishing that this ameloblast product is a constituent of the structure. Because Amtn does not present any canonical integrin-binding motif [RGD (Arg-Gly-Asp)], its targeting and persistence along the surface of the ameloblasts must be determined by other still unidentified portions of the molecule. One of those might be the phosphorylation and/or sugars attached to the protein, which would be consistent with the glycoconjugate-rich nature of the basal lamina [15,16]. Another line of evidence suggesting that Amtn is intimately associated with the enamel surface is its detection both on the basal lamina and on the surface of the enamel matrix at sites where the latter 'artefactually' separates from the ameloblasts. One intriguing possibility is that Amtn might serve as a bridging molecule that makes the ameloblasts adhere tightly to the mineral of enamel.

The second prominent localization of Amtn is at the interface between the gingiva and the mature tooth surface. The part of the gingiva that forms a tight seal around the tooth to protect the underlying periodontal tissues from exogenous unwanted molecules and bacteria originating from the oral cavity is called the JE [38,39]. The JE is a non-keratinized stratified epithelium whose innermost cell layer binds to the tooth through an internal basal lamina positioned similarly to that of maturation stage ameloblasts. Only the cells of the innermost layer stain for Amtn, which accumulates at the interface with the tooth where the basal lamina is found. The detection of *Amtn* expression in the mouse gingiva by RT–PCR suggests that the protein is being produced *in situ* and is not simply a carry-over from the reduced EO. Whether Amtn produced by the EO and JE has a similar adhesive role is still unknown. Certainly Amtn may represent, together with other proteins such as laminin-5 that is also expressed by ameloblasts [13,14], specific markers of the internal basal lamina of JE [37].

In conclusion, we have presented detailed expression and immunolocalization analyses of the newly discovered *Amtn* gene and its encoded protein. The main challenge now will be to ascribe a more direct functional role for this protein. Overexpression and/or ablation of this gene in the animal should perturb the tooth environment and provide clues as to the function it serves under normal or diseased states. Because Amtn is unique, such experiments are unlikely to be confounded by compensating mechanisms, at least by closely related family members.

This work was supported by the Canadian Institutes of Health Research (A.N., C.E.S. and R.St-A.) and the National Institute of Dental and Craniofacial Research grant DE12879 (J.T.W.). We are grateful to Micheline Fortin and Sylvia Francis Zalzal for their expert technical assistance with immunolabelling.

REFERENCES

1 Gibson, C. W. (1999) Regulation of amelogenin gene expression. Crit. Rev. Eukaryot. Gene Expr. **9**, 45–57
2 Nanci, A., Zalzal, S., Lavoie, P., Kunikata, M., Chen, W., Krebsbach, P. H., Yamada, Y., Hammarstrom, L., Simmer, J. P., Fincham, A. G. et al. (1998) Comparative immunochemical analyses of the developmental expression and distribution of ameloblastin and amelogenin in rat incisors. J. Histochem. Cytochem. **46**, 911–934
3 Smith, C. E. (1998) Cellular and chemical events during enamel maturation. Crit. Rev. Oral Biol. Med. **9**, 128–161
4 Kawasaki, K. and Weiss, K. M. (2003) Mineralized tissue and vertebrate evolution: the secretory calcium-binding phosphoprotein gene cluster. Proc. Natl. Acad. Sci. U.S.A. **100**, 4060–4065
5 Moradian-Oldak, J., Paine, M. L., Lei, Y. P., Fincham, A. G. and Snead, M. L. (2000) Self-assembly properties of recombinant engineered amelogenin proteins analyzed by dynamic light scattering and atomic force microscopy. J. Struct. Biol. **131**, 27–37
6 Dunglas, C., Septier, D., Paine, M. L., Zhu, D. H., Snead, M. L. and Goldberg, M. (2002) Ultrastructure of forming enamel in mouse bearing a transgene that disrupts the amelogenin self-assembly domains. Calcif. Tissue Int. **71**, 155–166
7 Paine, M. L., White, S. N., Luo, W., Fong, H., Sarikaya, M. and Snead, M. L. (2001) Regulated gene expression dictates enamel structure and tooth function. Matrix Biol. **20**, 273–292
8 Paine, M. L., Luo, W., Zhu, D. H., Bringas, Jr, P. and Snead, M. L. (2003) Functional domains for amelogenin revealed by compound genetic defects. J. Bone Miner. Res. **18**, 466–472
9 Gibson, C. W., Yuan, Z. A., Hall, B., Longenecker, G., Chen, E., Thyagarajan, T., Sreenath, T., Wright, J. T., Decker, S., Piddington, R. et al. (2001) Amelogenin-deficient mice display an amelogenesis imperfecta phenotype. J Biol. Chem. **276**, 31871–31875
10 Fukumoto, S., Kiba, T., Hall, B., Iehara, N., Nakamura, T., Longenecker, G., Krebsbach, P. H., Nanci, A., Kulkarni, A. B. and Yamada, Y. (2004) Ameloblastin is a cell adhesion molecule required for maintaining the differentiation state of ameloblasts. J. Cell Biol. **167**, 973–983
11 Masuya, H., Shimizu, K., Sezutsu, H., Sakuraba, Y., Nagano, J., Shimizu, A., Fujimoto, N., Kawai, A., Miura, I., Kaneda, H. et al. (2005) Enamelin (Enam) is essential for amelogenesis: ENU-induced mouse mutants as models for different clinical subtypes of human amelogenesis imperfecta (AI). Hum. Mol. Genet. **14**, 575–583
12 Stephanopoulos, G., Garefalaki, M. E. and Lyroudia, K. (2005) Genes and related proteins involved in amelogenesis imperfecta. J. Dent. Res. **84**, 1117–1126
13 Ryan, M. C., Lee, K., Miyashita, Y. and Carter, W. G. (1999) Targeted disruption of the LAMA3 gene in mice reveals abnormalities in survival and late stage differentiation of epithelial cells. J. Cell Biol. **145**, 1309–1323
14 Yoshiba, N., Yoshiba, K., Aberdam, D., Meneguzzi, G., Perrin-Schmitt, F., Stoetzel, C., Ruch, J. V. and Lesot, H. (1998) Expression and localization of laminin-5 subunits in the mouse incisor. Cell Tissue Res. **292**, 143–149
15 Nanci, A., Zalzal, S. and Smith, C. E. (1987) Application of backscattered electron imaging and lectin-gold cytochemistry to visualize the distribution of glycoconjugates in a basal lamina. Scanning Microsc. **1**, 1963–1970
16 Nanci, A., Zalzal, S. and Kogaya, Y. (1993) Cytochemical characterization of basement membranes in the enamel organ of the rat incisor. Histochemistry **99**, 321–331
17 Moffatt, P., Smith, C. E., Sooknanan, R., St-Arnaud, R. and Nanci, A. (2006) Identification of secreted and membrane proteins in the rat incisor enamel organ using a signal-trap screening approach. Eur. J. Oral Sci. **114** (Suppl. 1), 139–146
18 Smith, C. E., Nanci, A. and Moffatt, P. (2006) Evidence by signal peptide trap technology for expression of carbonic anhydrase 6 in rat incisor enamel organ. Eur. J. Oral Sci. **114** (Suppl. 1), 147–153
19 Rijnkels, M., Elnitski, L., Miller, W. and Rosen, J. M. (2003) Multispecies comparative analysis of a mammalian-specific genomic domain encoding secretory proteins. Genomics **82**, 417–432
20 Solomon, A., Murphy, C. L., Weaver, K., Weiss, D. T., Hrncic, R., Eulitz, M., Donnell, R. L., Sletten, K., Westermark, G. and Westermark, P. (2003) Calcifying epithelial odontogenic (Pindborg) tumor-associated amyloid consists of a novel human protein. J. Lab. Clin. Med. **142**, 348–355
21 Kawasaki, K. and Weiss, K. M. (2006) Evolutionary genetics of vertebrate tissue mineralization: the origin and evolution of the secretory calcium-binding phosphoprotein family. J. Exp. Zool. B Mol. Dev. Evol. **306**, 295–316
22 Iwasaki, K., Bajenova, E., Somogyi-Ganss, E., Miller, M., Nguyen, V., Nourkeyhani, H., Gao, Y., Wendel, M. and Ganss, B. (2005) Amelotin – a novel secreted, ameloblast-specific protein. J. Dent. Res. **84**, 1127–1132
23 Church, G. M. and Gilbert, W. (1984) Genomic sequencing. Proc. Natl. Acad. Sci. U.S.A. **81**, 1991–1995
24 Bendtsen, J. D., Nielsen, H., von, H. G. and Brunak, S. (2004) Improved prediction of signal peptides: SignalP 3.0. J. Mol. Biol. **340**, 783–795
25 Moffatt, P., Salois, P., St-Amant, N., Gaumond, M. H. and Lanctot, C. (2004) Identification of a conserved cluster of skin-specific genes encoding secreted proteins. Gene **334**, 123–131
26 Birney, E., Andrews, D., Caccamo, M., Chen, Y., Clarke, L., Coates, G., Cox, T., Cunningham, F., Curwen, V., Cutts, T. et al. (2006) Ensembl 2006. Nucleic Acids Res. **34**, D556–D561
27 Fisher, L. W. and Fedarko, N. S. (2003) Six genes expressed in bones and teeth encode the current members of the SIBLING family of proteins. Connect. Tissue Res. **44** (Suppl. 1), 33–40
28 Huq, N. L., Cross, K. J., Ung, M. and Reynolds, E. C. (2005) A review of protein structure and gene organisation for proteins associated with mineralised tissue and calcium phosphate stabilisation encoded on human chromosome 4. Arch. Oral Biol. **50**, 599–609
29 Zhang, Z. and Henzel, W. J. (2004) Signal peptide prediction based on analysis of experimentally verified cleavage sites. Protein Sci. **13**, 2819–2824
30 Kreegipuu, A., Blom, N. and Brunak, S. (1999) PhosphoBase, a database of phosphorylation sites: release 2.0. Nucleic Acids Res. **27**, 237–239
31 Gupta, R., Birch, H., Rapacki, K., Brunak, S. and Hansen, J. E. (1999) O-GLYCBASE version 4.0: a revised database of O-glycosylated proteins. Nucleic Acids Res. **27**, 370–372
32 Julenius, K., Molgaard, A., Gupta, R. and Brunak, S. (2005) Prediction, conservation analysis, and structural characterization of mammalian mucin-type O-glycosylation sites. Glycobiology **15**, 153–164
33 Elhammer, A. P., Poorman, R. A., Brown, E., Maggiora, L. L., Hoogerheide, J. G. and Kezdy, F. J. (1993) The specificity of UDP-GalNAc:polypeptide *N*-acetylgalactosaminyltransferase as inferred from a database of *in vivo* substrates and from the *in vitro* glycosylation of proteins and peptides. J. Biol. Chem. **268**, 10029–10038
34 Gericke, A., Qin, C., Spevak, L., Fujimoto, Y., Butler, W. T., Sorensen, E. S. and Boskey, A. L. (2005) Importance of phosphorylation for osteopontin regulation of biomineralization. Calcif. Tissue Int. **77**, 45–54
35 He, G., Ramachandran, A., Dahl, T., George, S., Schultz, D., Cookson, D., Veis, A. and George, A. (2005) Phosphorylation of phosphophoryn is crucial for its function as a mediator of biomineralization. J. Biol. Chem. **280**, 33109–33114
36 Tartaix, P. H., Doulaverakis, M., George, A., Fisher, L. W., Butler, W. T., Qin, C., Salih, E., Tan, M., Fujimoto, Y., Spevak, L. and Boskey, A. L. (2004) *In vitro* effects of dentin matrix protein-1 on hydroxyapatite formation provide insights into *in vivo* functions. J. Biol. Chem. **279**, 18115–18120
37 Oksonen, J., Sorokin, L. M., Virtanen, I. and Hormia, M. (2001) The junctional epithelium around murine teeth differs from gingival epithelium in its basement membrane composition. J. Dent. Res. **80**, 2093–2097
38 Bosshardt, D. D. and Lang, N. P. (2005) The junctional epithelium: from health to disease. J. Dent. Res. **84**, 9–20
39 Shimono, M., Ishikawa, T., Enokiya, Y., Muramatsu, T., Matsuzaka, K., Inoue, T., Abiko, Y., Yamaza, T., Kido, M. A., Tanaka, T. and Hashimoto, S. (2003) Biological characteristics of the junctional epithelium. J. Electron Microsc. (Tokyo) **52**, 627–639

Received 3 May 2006/14 June 2006; accepted 21 June 2006
Published as BJ Immediate Publication 21 June 2006, doi:10.1042/BJ20060662